Proceedings of the 31st International Symposium on Power Semiconductor Devices & ICs
May 19-23, 2019, Shanghai, China

Integrated GaN MIS-HEMT with Multi-Channel Heterojunction SBD Structures

Sheng Li, Siyang Liu, Chi Zhang, Jiaxing Wei,
Long Zhang, Weifeng Sun*
National ASIC System Engineering Research Center
Southeast University
Nanjing, China
*E-mail: swffrog@seu.edu.cn

Youhua Zhu, Tingting Zhang, Dongsheng
Wang, Yinxia Sun, Yiheng Li, Tinggang Zhu
CorEnergy Semiconductor Co., LTD
Zhangjiagang, China

***Abstract*—In this paper, the integrated GaN metal-insulator-semiconductor high electron mobility transistor (MIS-HEMT) with multi-channel heterojunction Schottky barrier diode (SBD) structures are proposed. By growing HEMT upon multi-channel heterojunction SBD with a polarization effect-free AlN insertion layer between them, the reverse conduction voltage (V_{R_F}) are decreased by 41% compared with traditional MIS-HEMT device. Meanwhile, the blocking characteristic is excellent and the forward conduction performances are maintained. On the other hand, the proposed device needs a relatively simple manufacturing process and the wafer area efficiency is relatively high.**

Keywords—reverse conduction, integrated structures, multi-channel

I. INTRODUCTION

GaN-based power devices become expected to renovate the traditional power systems to improve the conversion efficiency [1][2]. More and more GaN devices are applied to power electronic systems with bridge circuit topology or LLC resonant circuit topology (seen in Fig. 1)[3]-[5]. In these applications, it is inevitable for GaN devices to work at reverse conduction state. However, the reverse voltage drop (V_{R_F}) on the GaN devices with traditional structures is modulated by the gate bias and is usually even high, which brings higher energy loss and lower efficiency [6][7]. The above shortcomings become the obstacles in front of the developments of GaN devices.

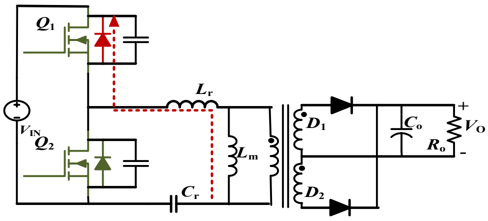

Fig. 1 LLC resonant circuit topology using GaN devices. The red line indicates the current path at freewheeling state.

The method that places anti-paralleled Schottky barrier diodes (SBDs) and high electron mobility transistor (HEMTs) into one chip is valid to reduce the high V_{R_F}. However, extra SBDs bring parasitic capacitances and inductances [8]. To minimize the parasitic values, an integrating way is required. Among previous approaches, the method that places a Schottky contact in the gate-to-drain region is compact [9][10], but the off-state leakage current is high. Also, an interdigitated metal-insulator-semiconductor (MIS) HEMT and SBD structure is proposed [11], but the wafer area efficiency is limited. In this work, the integrated GaN based MIS-HEMT with multi-channel heterojunction SBD structures are proposed to avoid the shortcomings. The investigation results show that the proposed devices exhibit low V_{R_F} and excellent blocking characteristics. Meanwhile, the forward conduction performances of the devices are maintained.

II. DEVICE STRUCTURE AND OPERATING PRINCIPLES

Fig. 2 shows the cross-section diagram of the proposed integrated MIS-HEMT with heterojunction SBD structures. The HEMT is grown upon heterojunction SBDs with a polarization effect-free AlN insertion layer between them. To maintain the electrical performances of the HEMT structure, the GaN buffer layer under the channel of HEMT (D_{ch1}) is relatively thick, which may make the polarization effect at SBD channel weaker and reduce the electron concentration. The polarization effect-free AlN layer is inserted between HEMT and SBD to maintain electron concentration in SBD channel. Once even lower V_{R_F} is required, multi-channel SBD structures can be applied to the device to achieve even lower reverse on-state resistance (R_{on_R}). To make the contacts, deep recesses should be made to access the barrier layer of SBDs. The drain contact is ohmic type, the gate contact is Schottky type, while the source contact is Schottky/ohmic mixed type. In this way, SBDs are integrated with the HEMT upon the same substrate efficiently.

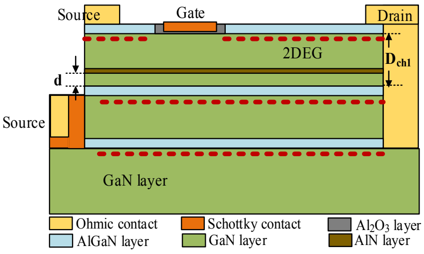

Fig. 2 The cross-section diagram of the integrated MIS-HEMT with heterojunction SBD structures

When applying the devices into the power systems, the basic operating principles are the same with traditional GaN MIS-HEMT devices, however, the reverse conduction capability is improved. At reverse conduction state, the gate to source voltage (V_{gs}) is usually 0V to −3V, while drain to source is reverse biased ($V_{ds}<0$). Under these bias conditions, three reverse current channels (Fig. 3(a)) are formed, resulting

978-1-7281-0581-9/19/$31.00 ©2019 IEEE

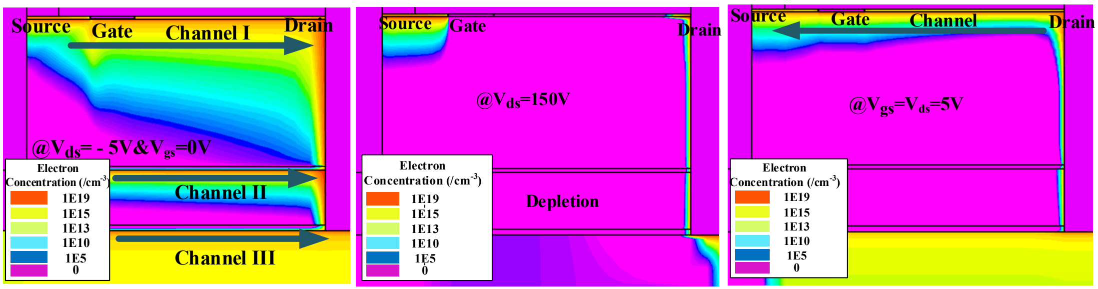

(a) (b) (c)

Fig. 3 The proposed device at different working state. (a) The electrons distribution of the device at reverse conduction state. (b) The electrons distribution at blocking state. (c) The electrons distribution of the device at forward conduction state.

in a lower V_{R_F} (decreased by 41% at 0V gate bias compared with original MIS-HEMT). At blocking state, the V_{gs} is still 0V to −3V but the V_{ds} is highly forward biased. Under these bias conditions, the Schottky gate and Schottky source help each other deplete the electrons (Fig. 3(b)), improving the breakdown voltage (BV, increased by 58%). At forward conduction state, the V_{gs} and V_{ds} are both forward biased, under these bias conditions, the forward conduction performances of the device are maintained since the forward current channel stays the same (Fig .3(c)).

III. ELECTRICAL PERFORMANCE OPTIMIZATION

The electrical performances of the proposed device together with the influences of layer depth and Schottky metal work-function have been investigated. Fig. 4 shows the reverse conduction performances with different layer depth and work-function. The reverse conduction capability of proposed devices are much better than traditional MIS-HEMT devices. At reverse conduction state, the reverse turn-on voltage (V_{R_T}) of the device is determined by that of SBD, moreover, the R_{on_R} are much smaller than traditional device since the current paths are more. To achieve better performances, the structure parameters should be optimized. As seen in Fig. 4(a), when the metal work-function is confirmed, larger D_{ch1} and smaller d make lower V_{R_F}. These phenomena indicate that the layer depth should be appropriate to make sure that the polarization charge density at HEMT and SBD channels is maintained. The results presented in Fig. 4(b) indicate that lower metal work-function of Schottky contact makes the reverse turn-on voltage smaller when the layer depth is confirmed, for the SBDs are easier to be turned-on with lower metal work-function.

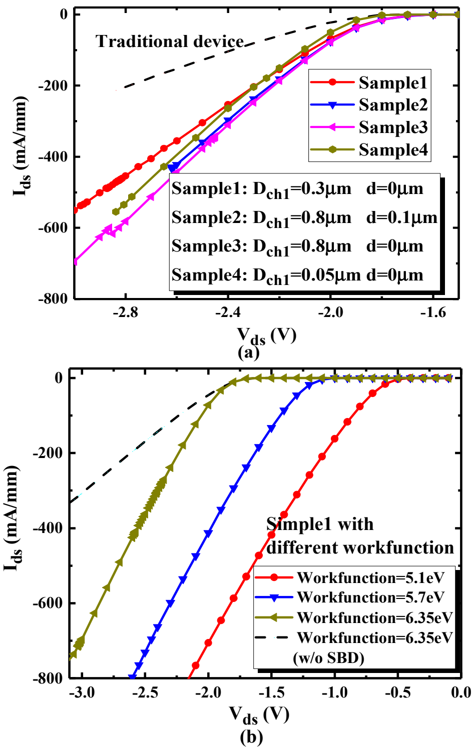

Fig. 4 The enhanced reverse conduction performances with different layer depth and Schottky metal work-function. (a)The reverse conduction performances of samples with the same Schottky metal work-function but different layer depth. (b) The reverse conduction performances with the same layer depth but different Schottky metal work-function.

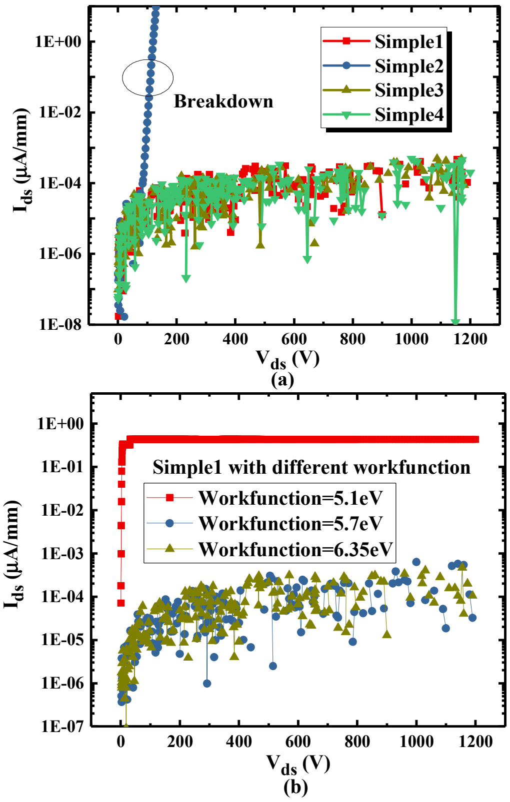

Fig. 5 The blocking characteristics of proposed devices (a) The blocking characteristics of the devices with different layer depth. (b) The blocking characteristics of sample1 with different work-function of the Shcottky metal.

Fig. 5 presents the blocking characteristics of different samples. As shown, sample2 (D_{ch1}=0.8μm, d=0.1μm) performs an extremely low BV. To find the mechanisms of this failure, more investigations have been accomplished. From Fig. 6(a) and (b), the drain to source leakage current mainly flows through the HEMT channel due to the high potential in the top GaN layer. The electron concentrations in the three AlGaN/GaN heterojunctions are extracted to understand this phenomenon. It can be seen from Fig. 6(c) that the larger D_{ch1} and d bring more electrons in channel II, conducting higher potential from drain to the top GaN layer. In this way, the BV of sample2 is reduced. Moreover, lower gate metal work-function also makes larger leakage current of the HEMT due to its weaker depletion capability on electrons in HEMT channel, as seen in Fig. 6(d). Thus, the position of insertion layer and metal work-function should be appropriate when designing the proposed devices.

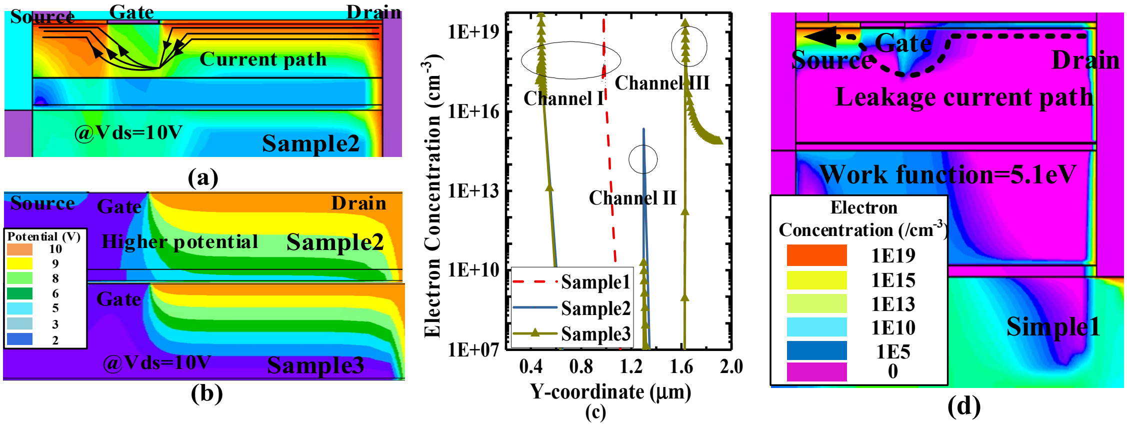

Fig. 6 Analyses on the devices under blocking state. (a) The leakage current path of simple2. (b) The potential distribution under the channels of simple2 and simple3. (c) The extracted electrons concentrations in channels at equilibrium. (d) The leakage current path of simple1 with gate metal work-function equaling to 5.1eV.

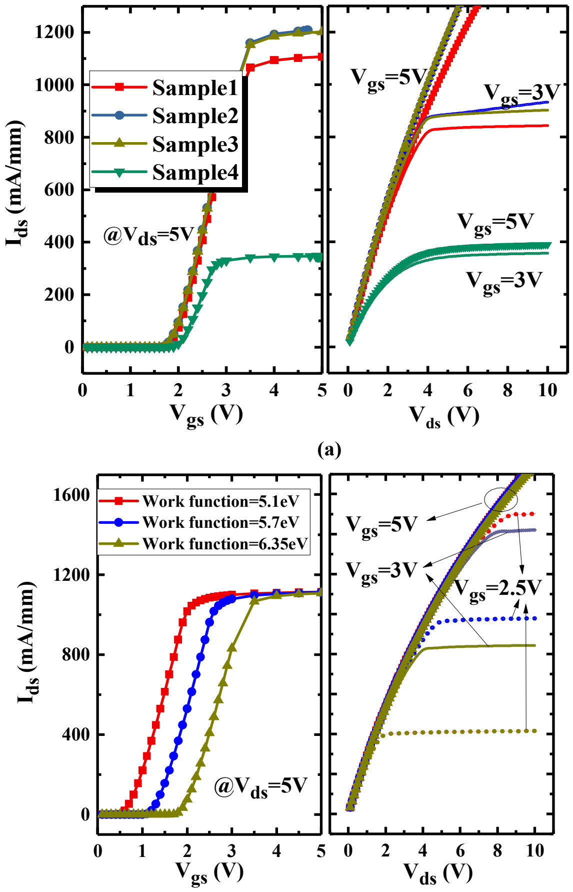

(a)

(b)

Fig. 7 The forward conduction performances of the proposed devices. (a) Influences of D_{ch1} and d on transfer and I-V characteristics. (b) Influences of Schottky metal work-function on transfer and I-V characteristics.

Also, the forward conduction performances of the proposed devices are presented in Fig. 7. The results indicate that D_{ch1} cannot impact the threshold voltage (V_{th}), however, smaller D_{ch1} can bring forward on-state resistance (R_{on}) increase even at high V_{gs}. These phenomena result from the narrowing of channel in HEMT structure, indicating that relatively thicker channel depth of HEMT is required to maintain the forward conduction performances. As for the influences of metal work-function, the V_{th} increases with the work-function, however, the R_{on} cannot be changed when the V_{gs} is high. Thus, thicker channel layer of HEMT and appropriate work-function are the key points to maintain the forward conduction performances.

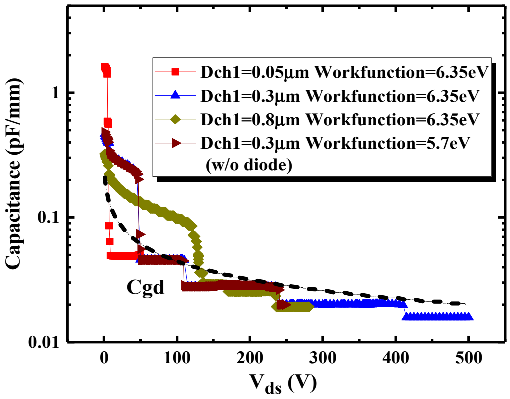

Fig. 8 Influences of D_{ch1} and Schottky metal work-function on capacitance characteristics

Reverse capacitance (C_{gd}) is an important parameter when estimating the switching performances of power devices. Fig. 8 presents the C_{gd} characteristics of different samples. The results show that the larger D_{ch1} make the reverse capacitance of the device larger at low V_{ds}, but the influences can be neglected at high V_{ds} under the same D_{ch1}. In conclusion, the C_{gd} of the proposed device is maintained at high V_{ds}.

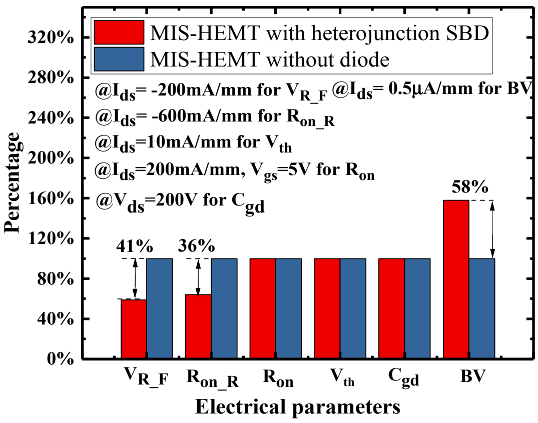

Fig. 9 Comparisons of the electrical parameters between the MIS-HEMT without diode (D_{ch1}=0.3mm) and MIS-HEMT with heterojunction SBD (D_{ch1}=0.3mm, d=0). The work-function for gate metal is 6.35eV, and the work-function for Schottky source metal is 5.1eV.

After optimizing the structure parameters, the comparisons of the electrical parameters between the optimal proposed device and original MIS-HEMT are presented in Fig. 9. The integrated MIS-HEMT with heterojunction SBD structure exhibits enhanced reverse conduction characteristic and blocking characteristic without changing forward conduction characteristic, performed as BV increased from 545V to 860V, V_{R_F} decreased from 2.6V to 1.55V, and R_{on_R} decreased from 2.5Ω·mm to 1.61Ω·mm.

IV. CONCLUSIONS

In this paper, the integrated GaN MIS-HEMT with multi-channel heterojunction SBD structures are proposed. By growing HEMT upon heterojunction SBDs with a polarization effect-free AlN insertion layer between them, the reverse conduction characteristic is enhanced. After optimizing the layer depth and metal work-function of proposed devices, the results show that the V_{R_F} is decreased by 41%, R_{on_R} is decreased by 36% and BV is increased by 58% compared with the traditional MIS-HEMT, meanwhile, the forward conduction performances of the device are maintained.

ACKNOWLEDGMENT

This work was supported by the National Natural Science Foundation of China (61604038), the Foundation of State Key Laboratory of Wide-bandgap Semiconductor Power Electronics Devices (2017KF003), the Key R&D Plan of Jiangsu Province (BE2018082), and the Fundamental Research Funds for the Central Universities.

REFERENCES

[1] B. Liu, R. Ren, E. A. Jones, F. Wang, D. Costinett and Z. Zhang, "A Modulation Compensation Scheme to Reduce Input Current Distortion in GaN-Based High Switching Frequency Three-Phase Three-Level Vienna-Type Rectifiers," in *IEEE Transactions on Power Electronics*, vol. 33, no. 1, pp. 283-298, Jan. 2018.

[2] C. Yao *et al.*, "Adaptive Constant Power Control of MHz GaN-Based AC/DC Converters for Low Power Applications," in *IEEE Transactions on Industry Applications*, vol. 54, no. 3, pp. 2525-2533, May-June 2018.

[3] A. Hariya *et al.*, "Circuit Design Techniques for Reducing the Effects of Magnetic Flux on GaN-HEMTs in 5-MHz 100-W High Power-Density LLC Resonant DC-DC Converters," in *IEEE Transactions on Power Electronics*, vol. 32, no. 8, pp. 5953-5963, Aug. 2017.

[4] M. H. Ahmed, M. A. de Rooij and J. Wang, "High-Power Density, 900-W LLC Converters for Servers Using GaN FETs: Toward Greater Efficiency and Power Density in 48 V to 6V12 V Converters," in *IEEE Power Electronics Magazine*, vol. 6, no. 1, pp. 40-47, March 2019.

[5] T. Ou *et al.*, "A Novel Transformer Structure Used in a 1.4 MHz LLC Resonant Converter with GaNFETs," *2018 IEEE International Power Electronics and Application Conference and Exposition (PEAC)*, Shenzhen, 2018, pp. 1-5.

[6] T. Sun, X. Ren, Q. Chen, Z. Zhang and X. Ruan, "Reliability and efficiency improvement in LLC resonant converter by adopting GaN transistor," *2015 IEEE Applied Power Electronics Conference and Exposition (APEC)*, Charlotte, NC, 2015, pp. 2459-2463.

[7] S. Park and J. Rivas-Davila, "Power loss of GaN transistor reverse diodes in a high frequency high voltage resonant rectifier," *2017 IEEE Applied Power Electronics Conference and Exposition (APEC)*, Tampa, FL, 2017, pp. 1942-1945.

[8] R. Zhu *et al.*, "A split gate vertical GaN power transistor with intrinsic reverse conduction capability and low gate charge," *2018 IEEE 30th International Symposium on Power Semiconductor Devices and ICs (ISPSD)*, Chicago, IL, 2018, pp. 212-215.

[9] R. Reiner *et al.*, "Integrated reverse-diodes for GaN-HEMT structures," *2015 IEEE 27th International Symposium on Power Semiconductor Devices & IC's (ISPSD)*, Hong Kong, 2015, pp. 45-48.

[10] Park B. R. *et al.*, “Normally-Off AlGaN/GaN-on-Si Power Switching Device with Embedded Schottky Barrier Diode”. Applied Physics Express, 2013, 6(3):031001.

[11] J. Lei *et al.*, "An interdigitated GaN MIS-HEMT/SBD normally-off power switching device with low ON-resistance and low reverse conduction loss," *2017 IEEE International Electron Devices Meeting (IEDM)*, San Francisco, CA, 2017, pp. 25.2.1-25.2.4.